International Journal of Science and Research (IJSR)
ISSN: 2319-7064
Impact Factor 2025: 7.089

Spatio-Temporal Analysis of Land Surface Temperature Using Google Earth Engine (2002-2025): A Case Study of Amroha

Umesh Kumar[1], Mohammed Faiz[2]

[1]Assistant Professor, Department of Geography, J. S. Hindu (P. G.) College, Amroha, India
Corresponding Author Email: *uumeshkumar58[at]gmail.com*

[2]Research Scholar, Interdisciplinary Department of Remote Sensing and GIS Applications, Aligarh Muslim University, Aligarh, India
Email: *faiz5225[at]gmail.com*

Abstract: ***Rapid urban and industrial growth in small towns of the Indo-Gangetic Plain has altered local thermal environments and vegetation cover. This study presents a Spatio-temporal analysis of Land Surface Temperature (LST), Normalized Difference Vegetation Index (NDVI), and Normalized Difference Built-up Index (NDBI) for Amroha town, Uttar Pradesh, India, using multi-temporal Landsat satellite imagery processed on the Google Earth Engine (GEE) cloud platform. LST, NDVI, and NDBI were derived for 2002, 2015 and 2025 using the mono-window / single-channel algorithm and standard spectral index formulations. Results indicate that mean LST rose from 32.8366 °C to 37.3483 °C while mean NDVI declined from 0.4530 to 0.3348 and mean NDBI increased from −0.0241 to 0.0076. Between 2002 and 2025, NDVI showed a declining trend of 0.1182 while NDBI showed an increasing trend of 0.0317, accompanied by an LST rise of 4.51 °C. Correlation analysis revealed a strong positive correlation (r^2= 0.871) between NDBI and LST, and a strong negative correlation (r^2= −0.832) between NDVI and LST. The findings underscore the utility of GEE as an efficient, cloud-based platform for rapid, long-term thermal monitoring of small urban centres and provide a baseline for understanding vegetation-built-up-temperature dynamics in Amroha.***

Keywords: Land Surface Temperature; Google Earth Engine; Amroha; Urban Heat Island; Landsat; Spatio-temporal Analysis; NDVI; NDBI

1. Introduction

Rapid and unplanned urban expansion is one of the most visible manifestations of land transformation in developing countries, and it exerts a measurable influence on local and regional thermal environments (Weng, 2009). The replacement of natural vegetation and open land with impervious surfaces such as concrete, asphalt, and rooftops alters the surface energy balance, reducing evapotranspiration and increasing sensible heat flux, which in turn elevates Land Surface Temperature (LST), a phenomenon widely studied as the Urban Heat Island (UHI) effect (Voogt & Oke, 2003).

LST is a key variable in the physics of land-surface processes at local through global scales, combining the results of all surface–atmosphere interactions and energy exchanges (Sobrino et al., 2004). Thermal remote sensing, particularly using Landsat Thematic Mapper (TM), Enhanced Thematic Mapper Plus (ETM+), and Thermal Infrared Sensor (TIRS) data, has been extensively used to derive LST at moderate spatial resolution over multiple decades (Jiménez-Muñoz & Sobrino, 2003; Avdan & Jovanovska, 2016).

Traditional processing of long time-series satellite data for LST retrieval is computationally intensive and requires substantial local storage and processing capability. The advent of the Google Earth Engine (GEE) cloud-computing platform has removed this barrier by providing free access to petabyte-scale satellite archives along with parallelized cloud processing, enabling rapid, reproducible, multi-temporal geospatial analysis (Gorelick et al., 2017). GEE has since been widely adopted for vegetation monitoring, built-up mapping, and LST/UHI studies across the globe.

While metropolitan cities such as Delhi, Lucknow, and Moradabad have received considerable research attention with respect to urban thermal dynamics, small and rapidly industrializing towns such as Amroha, a growing industrial and trading centre in Amroha district, Uttar Pradesh, remain comparatively understudied despite facing similar pressures from unplanned built-up expansion, brick-kiln and industrial activity, and loss of vegetation cover. This study therefore aims to: (i) retrieve and map multi-temporal LST, NDVI, and NDBI for Amroha using GEE; (ii) analyse the spatio-temporal change/trend in each of these three variables over the study period; and (iii) examine the statistical relationship of LST with NDVI and with NDBI.

A growing body of literature has applied GEE-based workflows to LST assessment across Indian cities. Studies on cities such as Delhi, Ahmedabad, Lucknow, and Moradabad have consistently reported an inverse relationship between vegetation cover (NDVI) and surface temperature, and a direct relationship between built-up density (NDBI) and LST (Avdan & Jovanovska, 2016). However, most of these studies focus on large metropolitan agglomerations with populations in the millions, where thermal anomalies are driven by dense high-rise construction, heavy traffic load, and extensive impervious cover. Comparatively little attention has been paid to Tier-3/Tier-4 towns and industrial satellite towns such as Amroha, even though such towns are undergoing some of the fastest rates of unplanned peri-urban and industrial land conversion in the Indo-Gangetic Plain, and their smaller size makes them more tractable for a detailed, high-resolution spatio-temporal analysis of the vegetation–built-up–temperature relationship.

2. Study Area

Amroha is a town and Nagar Palika Parishad located in Amroha district, in the western part of Uttar Pradesh, India, situated along National Highway NH 24. It lies approximately between 28°54′15.95″N latitude and 78°28′3.10″E longitude, covering a geographical area of about 1005 sq. km. The study area experiences a humid subtropical climate with hot summers, a monsoon season, and cool winters, with mean annual rainfall of approximately 391 mm and temperature ranging from 9 °C to 43 °C. The town has witnessed notable industrial growth (including paper and chemical industries) and consequent built-up expansion over the past two decades, making it a suitable site for examining vegetation loss, built-up growth, and surface thermal dynamics through NDVI, NDBI, and LST.

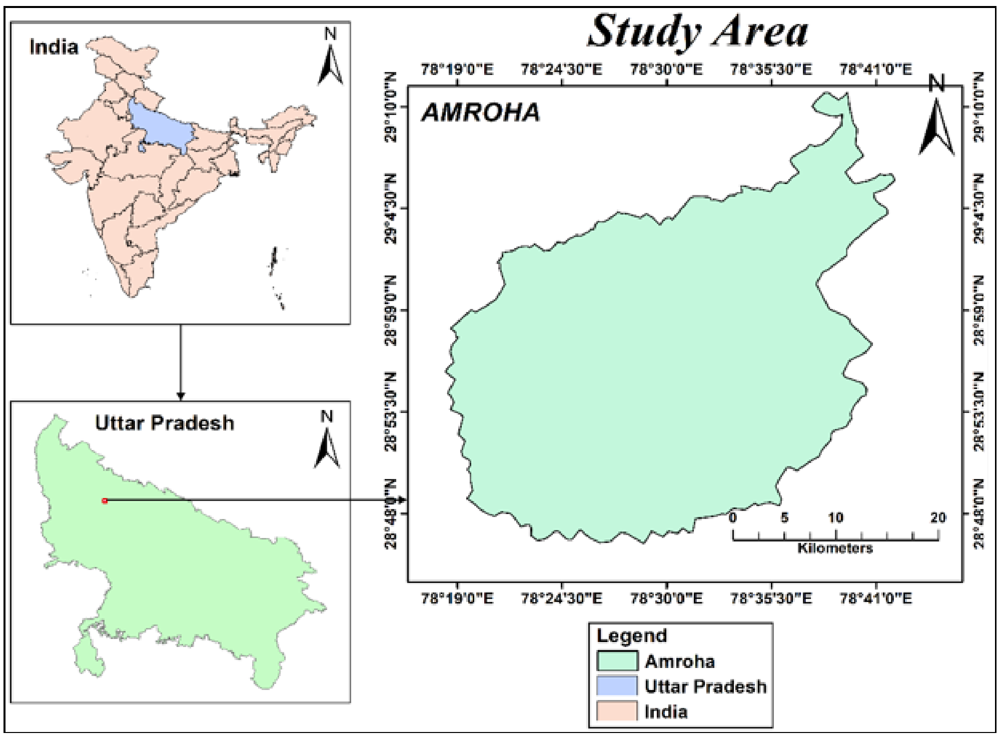

Figure 1: Location map of the study area

3. Data and Methodology

3.1 Data Used

Cloud-free Landsat satellite imagery (path/row: 145/40) was acquired for the months of March–May, representing peak pre-monsoon summer for the reference years 2002 (Landsat 5 TM), 2015 (Landsat 8 OLI/TIRS), 2025 (Landsat 9 OLI/TIRS). All datasets were accessed as USGS Collection-2, Level-2 Surface Reflectance and Surface Temperature products directly within the GEE data catalogue, which are already atmospherically corrected and radiometrically calibrated (USGS, 2021).

Table 1: Details of satellite data used in the study

Year	Satellite/Sensor	Path/Row	Acquisition Date	Spatial Resolution
2002	Landsat 5 TM	145/40	March–May 2002	30 m (Multispectral), 120 m (Thermal; resampled to 30 m)
2015	Landsat 8 OLI/TIRS	145/40	March–May 2002	30 m (Multispectral), 100 m (Thermal; resampled to 30 m)
2025	Landsat 9 OLI/TIRS	145/40	March–May 2002	30 m (Multispectral), 100 m (Thermal; resampled to 30 m)

3.2 Google Earth Engine Workflow

All pre-processing and analysis were carried out on the GEE JavaScript/Python API. The general workflow comprised: (i) definition of the Area of Interest (AOI) for Amroha; (ii) filtering of the Landsat image collection by date, path/row, and cloud cover (< 10 %); (iii) cloud/shadow masking using the QA_PIXEL band; (iv) computation of spectral indices (NDVI, NDBI); (v) retrieval of LST from the thermal band(s); and (vi) export of raster outputs for trend and statistical analysis in GIS software/ statistical software, e.g., ArcGIS Pro, QGIS, or Excel.

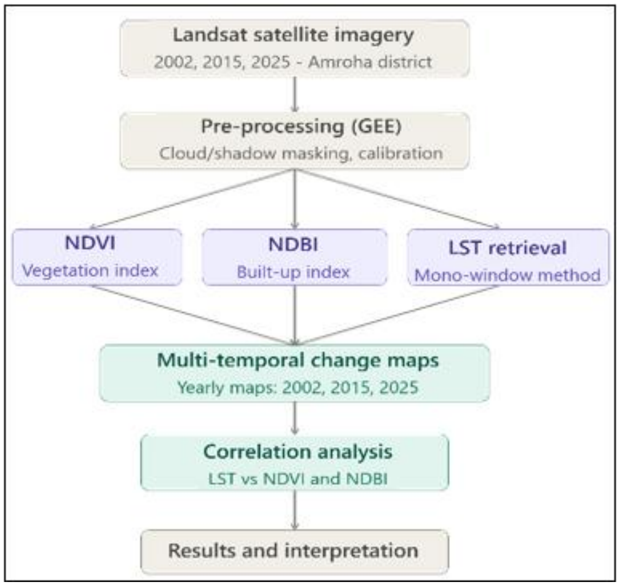

Figure 2: Methodological flowchart

3.3 NDVI and NDBI

The Normalized Difference Vegetation Index (NDVI) was computed as (Rouse et al., 1974):
NDVI = (NIR − RED) / (NIR + RED)
The Normalized Difference Built-up Index (NDBI) was computed as (Zha et al., 2003):
NDBI = (SWIR − NIR) / (SWIR + NIR)

3.4 LST Retrieval

LST was derived from the Landsat thermal band using the mono-window algorithm of Qin et al. (2001) / single-channel algorithm of Jiménez-Muñoz & Sobrino (2003). The Top-of-Atmosphere (TOA) spectral radiance was first converted to Brightness Temperature (BT), followed by correction for Land Surface Emissivity (LSE), which was estimated from NDVI using the Vegetation Cover Method / NDVI Threshold Method (Sobrino et al., 2004):

$$LST = BT / [1 + (\lambda \times BT / \rho) \times \ln(\varepsilon)]$$

where λ is the wavelength of emitted radiance, $\rho = h*c/\sigma$ (1.438×10^{-2} m K), and ε is the land surface emissivity. LST values were converted from Kelvin to degrees Celsius for interpretation.

3.5 Statistical Analysis

Descriptive statistics (mean, minimum, and maximum) were computed for LST, NDVI, and NDBI over the entire study area for each reference year to characterize their temporal trend. Pearson correlation coefficients were then calculated between LST and NDVI, and between LST and NDBI, on a pixel-wise basis for each year, to quantify the strength and direction of their spatial relationship across the study period.

4. Results and Discussion

4.1 Temporal Change in NDVI

NDVI maps (Figure 3) show a declining trend in vegetation greenness across Amroha over the study period. Mean NDVI decreased from 0.4530 in 2002 to 0.3348 in 2025 (Table 2), with the sharpest decline observed around the town core / industrial belt / peripheral agricultural land. The highest NDVI values (up to 0.8235) were consistently recorded over agricultural fields and riparian vegetation, while the lowest values (as low as −0.0029) occurred over built-up and bare/fallow surfaces.

Paper ID: SR26729204800 DOI: https://dx.doi.org/10.21275/SR26729204800

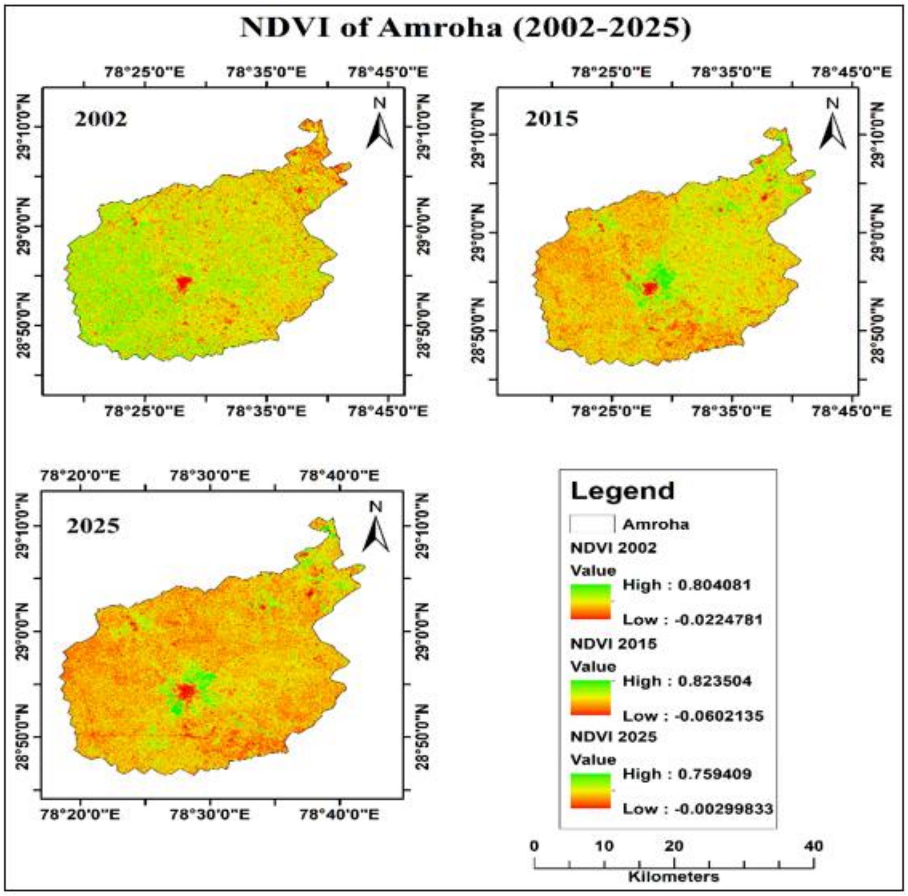

Figure 3: Multi-temporal NDVI distribution

Table 2: Year-wise NDVI statistics**.**

Year	Mean NDVI	Min NDVI	Max NDVI
2002	0.4530	−0.0224	0.8040
2015	0.4085	−0.0602	0.8235
2025	0.3348	−0.0029	0.7594

4.2 Temporal Change in NDBI

NDBI maps (Figure 4) show a rising trend in built-up/impervious surface signal over the study period. Mean NDBI increased from −0.0241 in 2002 to 0.0076 in 2025 (Table 3), with the most pronounced increase concentrated around the town core and industrial belt. This is consistent with the visually apparent densification of built-up cover evident in the false-colour composites for each reference year.

Paper ID: SR26729204800 DOI: https://dx.doi.org/10.21275/SR26729204800

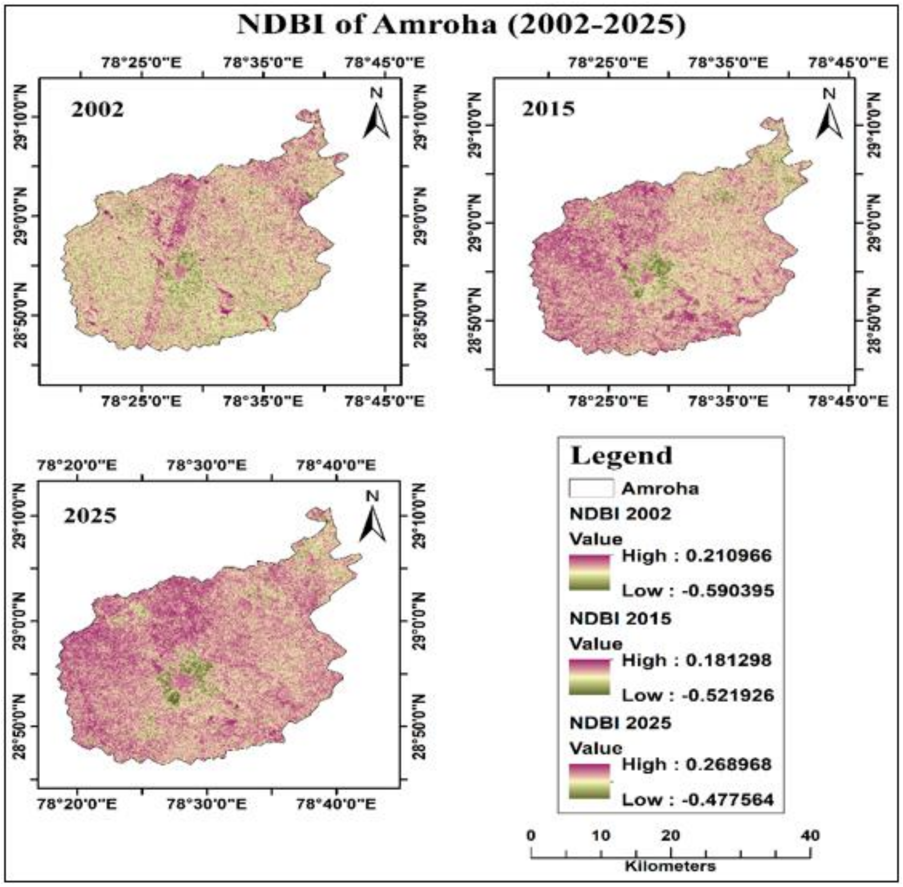

Figure 4: Multi-temporal NDBI distribution

Table 3: Year-wise NDBI statistics

Year	Mean NDBI	Min NDBI	Max NDBI
2002	−0.0241	−0.5903	0.2109
2015	−0.0173	−0.5219	0.1812
2025	0.0076	−0.4775	0.2689

4.3 Spatio-Temporal Pattern of LST

Retrieved LST maps (Figure 5) show a consistent pattern of higher surface temperatures over the built-up core and industrial belt of Amroha, with mean LST rising from 32.8366 °C in 2002 to 37.3483 °C in 2025 (Table 4). The highest LST values (up to 48.5529 °C) were recorded over industrial/commercial zones and exposed/bare surfaces, coinciding with areas of high NDBI, while the lowest values (as low as 25.9743 °C) were associated with water bodies and dense vegetation cover, coinciding with areas of high NDVI. This spatial coincidence points to a close visual association between rising LST and the NDVI/NDBI change patterns described above.

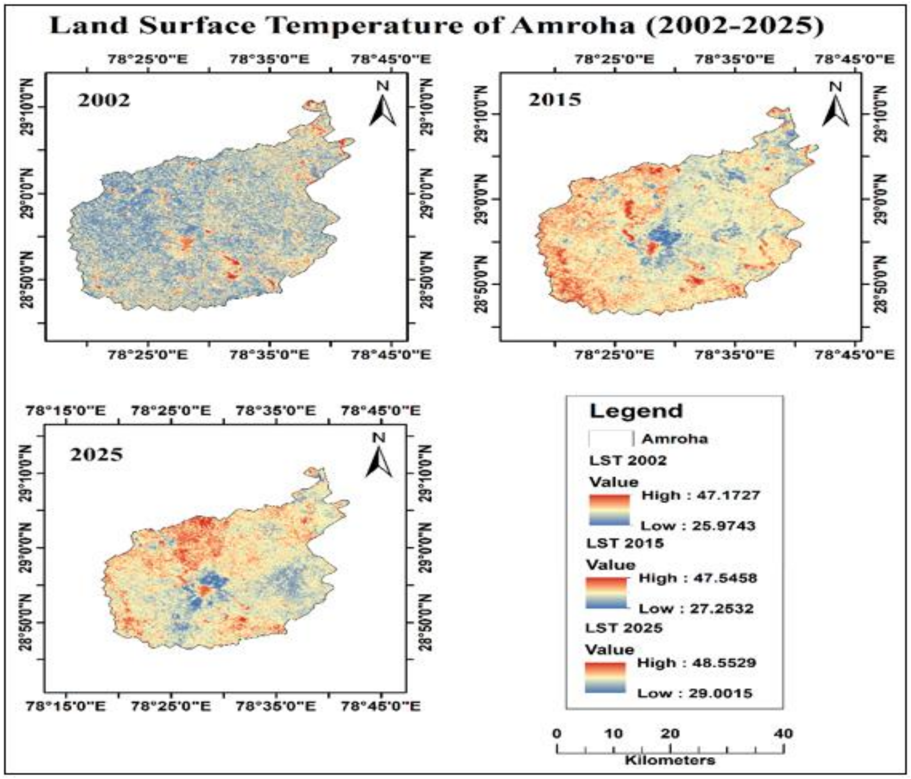

Figure 5: Multi-temporal LST distribution

Table 4: Year-wise LST statistics.

Year	Mean LST (°C)	Min LST (°C)	Max LST (°C)
2002	32.8366	25.9743	47.1727
2015	37.3153	27.2532	47.5458
2025	37.3483	29.0015	48.5529

4.4 Relationship between LST, NDVI, and NDBI

Pixel-wise correlation analysis (Table 5) between the three variables showed a strong positive correlation (r = 0.871) between LST and NDBI, and a strong negative correlation (r = −0.832) between LST and NDVI, in each of the reference years. The scatter plots (Figure 6) confirm that surface temperature consistently rises with increasing NDBI and falls with increasing NDVI, indicating that vegetation cover exerts a cooling influence while built-up/impervious surfaces intensify surface heating across the study period.

Table 5: Year-wise correlation coefficients of LST with NDVI and NDBI.

Year	r^2 (LST, NDVI)	r^2(LST, NDBI)
2025	0.871	−0.832

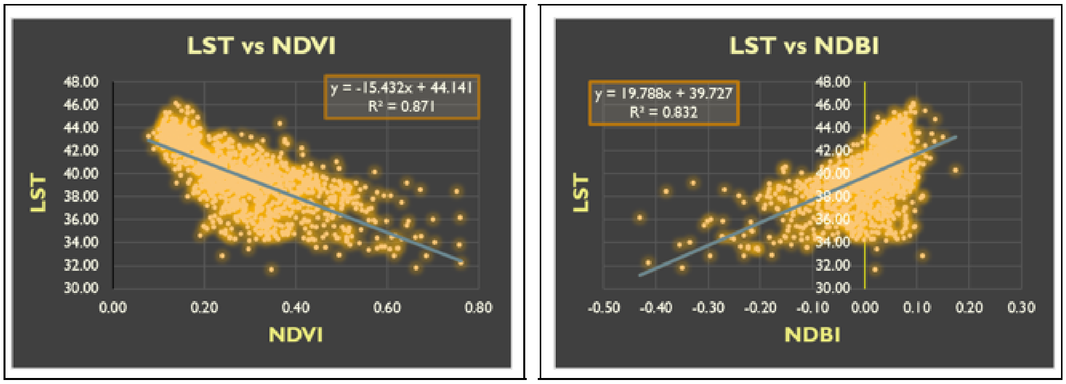

Figure 6: LST–NDVI and LST–NDBI correlation plots.

4.5 Discussion

The observed decline in NDVI, rise in NDBI, and consequent increase in LST in Amroha over the study period align with the broader trend of surface urban heat island intensification reported for small and medium Indian towns undergoing rapid, often unplanned, built-up expansion (Weng, 2009). The strong positive association between NDBI and LST, alongside the cooling effect indicated by the negative NDVI–LST correlation, reinforces the case for retaining green cover and water bodies as a heat-mitigation strategy. The results also demonstrate the practical value of GEE for enabling rapid, decadal-scale monitoring of vegetation, built-up, and thermal indices in data- and resource-constrained small-town contexts, where conventional desktop-based processing of large multi-temporal satellite archives is often impractical.

4.6 Limitations and Future Scope

This study, while demonstrating the utility of GEE for rapid multi-temporal LST retrieval, is subject to a few limitations. First, LST retrieved from Landsat thermal bands (30/100 m resampled resolution) cannot capture fine-scale intra-urban thermal variability that higher-resolution sensors (e.g., ECOSTRESS, ASTER) could reveal. Second, single-date, pre-monsoon imagery for each reference year may not fully represent seasonal and diurnal LST variability across the year. Third, the mono-window/single-channel algorithm used here assumes uniform atmospheric conditions and does not incorporate localized meteorological data (air temperature, humidity, wind speed), which could refine LST accuracy through ground validation. Future work on Amroha could incorporate multi-seasonal imagery, socio-economic and population density data, and ground-based temperature loggers to strengthen the NDVI/NDBI–LST relationship and better inform local heat-mitigation policy.

5. Conclusion

This study demonstrates the effectiveness of the Google Earth Engine platform for spatio-temporal analysis of LST, NDVI, and NDBI in Amroha, a rapidly urbanizing small town in Uttar Pradesh, India. Between 2002 and 2025, mean NDVI declined by 0.1182 and mean NDBI increased by 0.0317, accompanied by a mean LST rise of 4.51 °C. LST was found to be strongly positively correlated with NDBI and negatively correlated with NDVI, confirming the role of vegetation loss and built-up growth in driving local surface warming. These findings provide a scientific baseline for urban planners and local authorities in Amroha district to incorporate thermal considerations, such as green-space preservation and cool-roofing strategies into future planning for Amroha. Future research should extend this analysis using higher-resolution thermal sensors and incorporate diurnal and seasonal LST variability.

Acknowledgements
The authors extend their gratitude to the United States Geological Survey (USGS) for granting access to satellite data at no cost. The authors also extend their gratitude to Survey of India and Diva.gis portal. We also acknowledge the gratitude to the Department of Geography, J. S. Hindu (P. G.) College, Amroha. The authors would like to acknowledge the support received from the Interdisciplinary Department of Remote Sensing and GIS Applications at Aligarh Muslim University.

References

[1] Artis, D. A., & Carnahan, W. H. (1982). Survey of emissivity variability in thermography of urban areas. Remote Sensing of Environment, 12(4), 313–329.
[2] Avdan, U., & Jovanovska, G. (2016). Algorithm for automated mapping of land surface temperature using LANDSAT 8 satellite data. Journal of Sensors, 2016, Article 1480307.
[3] Chander, G., Markham, B. L., & Helder, D. L. (2009). Summary of current radiometric calibration coefficients for Landsat MSS, TM, ETM+, and EO-1 ALI sensors. Remote Sensing of Environment, 113(5), 893–903.
[4] Gorelick, N., Hancher, M., Dixon, M., Ilyushchenko, S., Thau, D., & Moore, R. (2017). Google Earth Engine: Planetary-scale geospatial analysis for everyone. Remote Sensing of Environment, 202, 18–27.
[5] Jiménez-Muñoz, J. C., & Sobrino, J. A. (2003). A generalized single-channel method for retrieving land surface temperature from remote sensing data. Journal of Geophysical Research, 108(D22), 4688.
[6] Qin, Z., Karnieli, A., & Berliner, P. (2001). A mono-window algorithm for retrieving land surface temperature from Landsat TM data and its application to the Israel–Egypt border region. International Journal of Remote Sensing, 22(18), 3719–3746.
[7] Rouse, J. W., Haas, R. H., Schell, J. A., & Deering, D. W. (1974). Monitoring vegetation systems in the Great Plains with ERTS. In Proceedings of the Third ERTS Symposium (Vol. 1, pp. 309–317). NASA SP-351.
[8] Sobrino, J. A., Jiménez-Muñoz, J. C., & Paolini, L. (2004). Land surface temperature retrieval from LANDSAT TM 5. Remote Sensing of Environment, 90(4), 434–440.
[9] USGS. (2021). Landsat Collection 2 Level-2 Science Products. U.S. Geological Survey, Earth Resources Observation and Science (EROS) Center.
[10] Voogt, J. A., & Oke, T. R. (2003). Thermal remote sensing of urban climates. Remote Sensing of Environment, 86(3), 370–384.
[11] Weng, Q. (2009). Thermal infrared remote sensing for urban climate and environmental studies: Methods, applications, and trends. ISPRS Journal of Photogrammetry and Remote Sensing, 64(4), 335–344.
[12] Zha, Y., Gao, J., & Ni, S. (2003). Use of normalized difference built-up index in automatically mapping urban areas from TM imagery. International Journal of Remote Sensing, 24(3), 583–594.